Int J Clin Exp Med 2015;8(8):12182-12191
www.ijcem.com /ISSN:1940-5901/IJCEM0008316

Original Article

Anti-tumor effect of RGD modified PTX loaded liposome on prostatic cancer

Yunjie Cao, Yaojun Zhou, Qianfeng Zhuang, Li Cui, Xianlin Xu, Renfang Xu, Xiaozhou He

Department of Urology, Third Affiliated Hospital of Soochow University, Changzhou 213003, China

Received March 22, 2015; Accepted July 2, 2015; Epub August 15, 2015; Published August 30, 2015

Abstract: In this study, we report an active targeting liposomal formulation directed by a novel peptide (RGD) that specifically binds to the integrins receptors overexpressed on prostatic cancer cells. The objectives of this study were to evaluate the in vitro and in vivo tumor drug targeting delivery of RGD modified liposomes on PC-3 cells and DU145 cells. The uptake efficiency of RGD-LP was 5.2 times higher than that of LP on PC-3 cells. The uptake efficiency of RGD-LP was 3.2 times higher than that of LP on DU145 cells. The anti-proliferative activity of RGD-LP-PTX against PC-3 cells and DU145 cells were much stronger compared to that of LP-PTX and free PTX, respectively. The tumor spheroids experiment revealed that RGD-LP-PTX was more efficaciously internalized into tumor spheroids than LP in both PC-3 cells and DU145 cells. Compared to LP-PTX and free PTX, RGD-LP-PTX showed the greatest tumor growth inhibitory effect *in vivo*. In brief, the RGD-LP may be an efficient targeting drug delivery system for prostatic cancer.

Keywords: Prostatic cancer, integrins receptors, liposome, tumor targeting

Introduction

Prostate cancer is a malignant tumor in male prostate tissues, resulting from abnormal and disordered growth of the acinar cells. The incidence of prostate cancer is significantly different in various geographic areas and races. In Western countries, prostate cancer is the most commonly seen malignant tumor, ranking first in mortality and second in morbidity among all malignant tumors [1]. In Asia, the incidence is lower, but it has been rising rapidly in recent years. According to statistics, there are 70 to 80 thousand new cases of prostate cancer each year in China, with 95% occurring in people aged 60 years and over. The incidence of prostate cancer increases constantly with age [2, 3]. With the population aging in China, the incidence and the number of patients with prostate cancer will continue to increase, possibly evolving into one of the first three malignant tumors in men [4]. Prostate cancer mainly occurs in the outer gland, mostly without any clinical symptoms in the early period, and it does not draw the patients' attention even though the tumor enlarges and compresses the urethra to cause discomfort, since it is often confused with prostatic hypertrophy. Therefore, early diagnosis of prostate cancer is at a low rate and the cancer in 80% patients is found out only after distant metastasis is detected [5, 6]. At this time, the disease is at its advanced stage, with poor prognosis. Various treatment methods have been proposed both at home and abroad. They can be classified as follows: endocrine treatment, mainly antiandrogens; chemotherapy, mainly mitoxantrone, estramustine phosphate, docetaxel and cabazitaxel; chemotherapy; immunotherapy, mainly with activated PAS activating the antigen-specific T cells; and traditional Chinese medicine improving immunity of the body [7-10]. At present, although there are various methods to treat androgen-independent prostate cancer, the efficacy is limited and radical cure is completely impossible, only alleviating the symptoms, improving the quality of life or prolonging the short-term survival. It is therefore urgent to explore the more effective methods to treat androgen-independent prostate cancer, with great value in clinical practice and a bright prospect for application.

In the last two decades, Sterically stabilized liposomes (SSL) (i.e., PEG-liposomes) were used to increase the accumulation of the encapsulated anticancer drugs into solid tumors by the process of targeting due to the effect of enhanced permeability and retention (EPR) [11, 12]. To achieve more specific targeting, the PEG-liposomes have been modified with various ligands [13-15]. These targeted PEG-liposomes demonstrated an improved therapeutic efficacy compared to non-targeted ones, whereas they showed less enhancement in tumor accumulation. Integrins are a family of cell adhesion molecules composed of two non-covalently associated chains [16, 17]. Both subunits, α and β, traverse the membrane and "integrate" the extracellular matrix with the intracellular compartment [18-20]. The RGD (Arg-Gly-Asp) sequence is known to serve as a recognition motif in multiple ligands for several different integrins [21]. Integrin-mediated cell attachment and internalization are exploited by a variety of bacteria and viruses for cell entry [22]. It is also suggested that the RGD-containing peptide can be internalized into cells by integrin-mediated endocytosis [23]. Recently, integrin-mediated carriers, such as RGD-modified liposomes, nanoparticles, conjugates, have been investigated as gene vehicles to enhance gene transfection [24-26]. It is reasonable that RGD-peptide could be used to modify the liposomes to facilitate the intracellular delivery of the entrapped anticancer agents.

Herein, RGD conjugated polyethylene glycol (PEG)-modified liposome (RGD-LP) was constructed as a nanoplatform to deliver PTX contrast agent targeting the tumor specifically, yielding RGD-LP-PTX. The targeting and anti-tumor efficiency in hepatocellular carcinoma of this contrast agent were evaluated in vitro and in vivo.

Materials and methods

Soybean lecithin consisting of 90-95% phosphatidylcholine and $mPEG_{2000}$-DSPE and $Mal\text{-}PEG_{2000}$-DSPE were purchased from Avanti lipid (USA). Cholesterol (CHO) was purchased from Nanjing Chemical Company (Nanjing, China). Coumarin-6 was purchased from Sigma (USA). Arginine-glycine-aspartic acid peptide (RGDyk) with terminal cysteine was synthesized according to the standard solid phase peptide synthesis by Shanghai Jier Bio-pharmaceutical Co., Ltd. Cell culture plates were purchased from corning Biotechnology Co. Ltd. (USA). Other chemicals and reagents were of analytical grade and obtained commercially.

BALB/c male athymic mice (about 20 g) were purchased from the Experiment Animal Center of Suzhou University (P.R. China). All of the animal experiments adhered to the principles of care and use of laboratory animals and were approved by the Experiment Animal Administrative committee of Suzhou University.

Preparation and characterization of liposome

RGD modified PTX loaded liposome (RGD-LP-PTX) were prepared by thin film hydration methods [27, 28]. Briefly, SPC, cholesterol, PTX (5% of the SPC + cholesterol weight), DSPE-PEG2000, DSPE-PEG3500-RGD were dissolved in chloroform (total molar ratio of phospholipid and cholesterol was 5:3, molar ratio of DSPE-PEG2000; DSPE-PEG3500-RGD was 9.2:0.8). Chloroform was then evaporated by rotary evaporation and residual organic solvent was removed in vacuum overnight. Then the thin film was hydrated in phosphate-buffered saline (PBS, pH 7.4) for 1 h at 37°C, followed by an intermittently probe sonication for 50 s at 100 W.

Coumarin-6 labeled liposomes were prepared with appropriate amount of Coumarin-6 added to the lipid organic solution and replace the PTX, respectively. The entrapment efficiency of PTX was determined by high performance liquid chromatography (Agilent 1100, USA). The mean size and zeta potential of LP-PTX, and RGD-LP-PTX were detected by Malvern Zetasizer Nano ZS90 (Malvern Instruments Ltd., UK).

In vitro PTX release study was performed with a dialysis method. PBS (pH 7.4) containing 0.1% (v/v) Tween 80 was used as the release media. PTX-loaded liposomes or free PTX were placed into dialysis tubes (MWCO8000 Da) and tightly sealed. The dialysis tubes were added into 50 ml release media and incubated at 37°C with gently oscillating for 72 h. At predetermined time points, 0.1 ml release media was sampled and replaced with equal volume of fresh release

Table 1. Characteristics of PTX-loaded LP and RGD-LP (*n*=3)

Group	Particle Size (nm)	Polydispersity	Zeta-potential (mV)	Encapsulation Efficiency (%)
LP-PTX	91±7.8	0.110	3.75±1.44	84.7±1.47
RGD-LP-PTX	95±6.4	0.142	-2.63±1.17	83.6±1.25

media. The samples were then analyzed by HPLC to determine the concentrations of PTX.

In vitro cellular uptake

PC-3 cells, DU145 cells and Hela cells were grown in RPMI-1640 medium (GIBCO) contains 10% FBS, 100 μg/mL streptomycin, and 100 U/mL penicillin. The cells were maintained at 37°C in a humidified incubator with 5% CO_2.

For quantitative study, PC-3 cells, DU145 cells and Hela cells (American Type Culture Collection) were harvested with 0.125% Gibcotrypsin-EDTA solution (Invitrogen) and seeded into 24 well assay plates (Corning Incorporated) at 10^5 viable cells/well. After the cells reached confluence, the cells were incubated with 100 uL of 10 μg/mL Coumarin-6 loaded liposomes (all three types) in the 1640 supplemented with 10% Hyclone fetal bovine serum (FBS, Thermo Scientific) and 1% Gibco penicillin-streptomycin (Invitrogen) at 37°C for 4 h. At designated time period, the suspension was removed and the wells were washed three times with 1000 μL cold PBS, and were trypsinized and resuspended in 0.4 mL PBS. The fluorescent intensity of cells was measured by a flow cytometer (Cytomics™ FC 500, Beckman Coulter, Miami, FL, USA) with the excitation wavelength at 465 nm and the emission wavelength at 502 nm. Ten thousand events were recorded for each sample.

To study the effect of different inhibitors on the cellular uptake of RGD-LP, the PC-3 cells were pre-incubated with different inhibitors for 30 min at 37°C. Amiloride (1.2 mg/mL), chlorpromazine (10 mg/mL), filipin (3 mg/mL) and free RGD peptide (20 mg/mL) were added respectively. To study the effect of temperature on the cellular uptake, the cells were incubated under both 37°C and 4°C. Then the inhibitor-containing culture media was discarded and coumarin-6 labeled liposome-containing culture media was applied for 4 h incubation. Then the cells were treated as the quantitative study described, and the fluorescence intensity was determined by flow cytometer (Cytomics™ FC 500, Beckman Coulter, Miami, FL, USA).

Cell proliferation assays

Cell proliferation was carried out using a Cell Counting Kit-8 (CCK-8, Dojindo Molecular Technologies) assay as previous descriptions [24]. Briefly cells were seeded in a 96-well plate at an initial density of 3000 cells per well. After different time intervals, 10 μl CCK-8 was added to each well for another 2 hour-incubation protected from light. The absorbance (Ab) at 450 nm was recorded by a micro-plate reader (Thermo Multiskan MK3, Thermo Scientifc) and cell viability was calculated as the following function:

$$\text{Cell viability\%} = \frac{(Ab_{Sample} - Ab_{Blank})}{(Ab_{Control} - Ab_{Blank})} \times 100\%$$

Where Ab_{sample}, $Ab_{control}$, and Ab_{blank} are the absorbance values of each sample, the cells cultured in culture medium without any additional substances, and the culture medium without cells in wells, respectively.

Tumor spheroid penetration and growth inhibition

To prepare the three-dimensional tumor spheroids, PC-3 cells and DU145 cells were seeded at a density of 2×10^3 cells/200 μL per well in 96-well plates coated by 80 μL of a 2% low-melting-temperature agarose. Seven days after the cells were seeded; tumor spheroids were treated with 10 μg/mL coumarin-6 loaded liposome. After 4 h of incubation, the spheroids were rinsed three times with ice-cold PBS and fixed by 4% paraformaldehyde for 30 min. Then, the spheroids were transferred to glass slides and covered by glycerophosphate. Fluorescent intensity was observed by laser scanning confocal microscopy (Leica, Germany).

Tumor spheroids were prepared as described above. Seven days later, wells containing spheroids were treated with 0.25 μg/mL of PTX solution, and PTX-loaded liposomes. The length and width of each spheroid were measured every day for 7 days. The volume was calculated. A volume curve was drawn to compare the effect of each treatment by the different formulations.

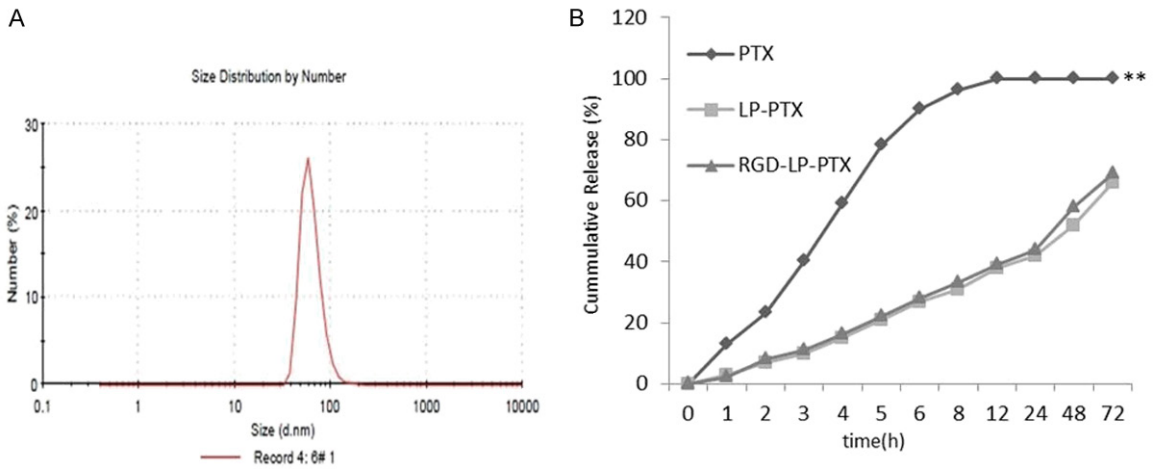

Figure 1. A. Size distribution graph of PTX-loaded RGD-LP. B. The PTX release profiles of free PTX, LP-PTX and RGD-LP-PTX in PBS over 72 h (n = 3, mean ± SD). Compare to LP and RGD-LP-PTX, $^{**}P < 0.01$.

In vivo tumor growth inhibition study

The PC-3 bearing mice xenograft models were established by injecting PC-3 cells (1×10^7 cells per animal, subcutaneous injection) into the back of 4-6 week-old BALB/c male athymic mice. Tumor volume (mm^3) was measured with vernier caliper. 40 mice with prostatic cancer xenograft models were divided into four groups. When the tumors reached 100-200 mm^3, the mice were administrated with saline, free PTX, LP-PTX, and RGD-LP-PTX, respectively. The drugs were administrated once every other day (totally 10 mg/kg) and the volumes of tumors were measured. The tumor inhibition rate was calculated by the formula as fellow,

Tumor inhibition rate = $(1 - V_t/V_0) \times 100\%$. V_t was the tumor volume of mice treated and V_0 was the initial tumor volume of mice untreated.

Statistical analysis

Analysis of variance (ANOVA) was used to check the variance of the whole values in each group. Statistical significance was evaluated by using Student's t-test for the comparisons of experimental groups.

Results

Physicochemical Properties of PTX-Loaded Liposomes

The particle size and polydispersity index (PDI) of liposomal samples were measured via a nanoparticle analyzer at 20°C with results given in **Table 1**. The size distribution graph of PTX-loaded RGD-LP was shown in **Figure 1A**. RGD-LP-PTX had a mean particle size about 95 nm with a PDI of 0.20, similar to that of the LP, Indicating homogeneity in their dispersion state. The encapsulation efficiency (EE) of PTX in the liposomes determined by HPLC was 83.6%, indicating that peptide modification did not affect PTX loading into the liposome.

Herein the *in vitro* release of PTX from the liposomes was investigated. **Figure 1B** shows the release profile of these two groups. Compared with the rapid release of free PTX, the two liposome groups exhibited similar and sustained release manners and no burst initial release was observed.

Cellular uptake

To investigate the selectivity and internalization of liposomes, the cellular uptake of different liposomes in PC-3 cells, DU145 cells and Hela cells were examined, Here Hela cells was used as negative cells without integrin express in the cells. As shown in **Figure 2**. In Hela cells, there was no significant difference between the cellular uptake of LP and RGD-LP. In PC-3 cells, RGD-LP uptake was about 5.2 times higher than that of LP, respectively. That was the result of the targeting capacity of integrin receptors expression in PC-3 cells. The cellular uptake results were consistent with the integrin expression levels on cell surface, indicating that the RGD motif had the ability to recognize and target integrin receptors expressed on the surface of cells. In DU145 cells, RGD-LP uptake was

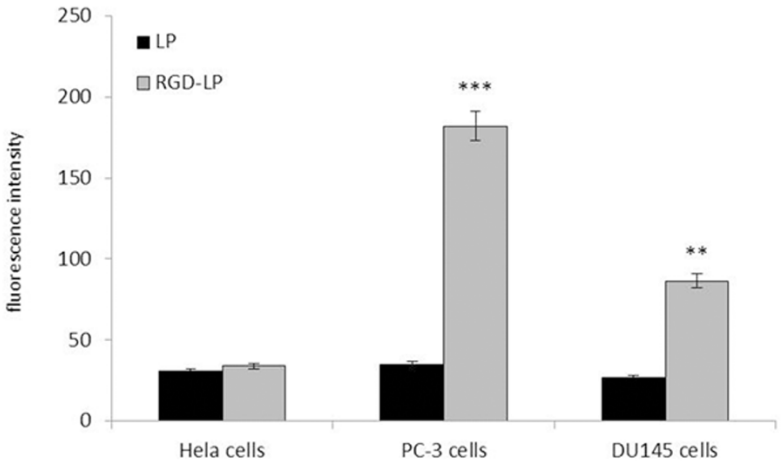

Figure 2. Measurement of *in vitro* uptake of coumarin-6 labeled liposomes by Hela cells, PC-3 cells and DU145 cells at 4 h. Data represented the mean ± SD, $n = 3$. Compare to LP, $^{**}P < 0.01$;$^{***}P < 0.001$.

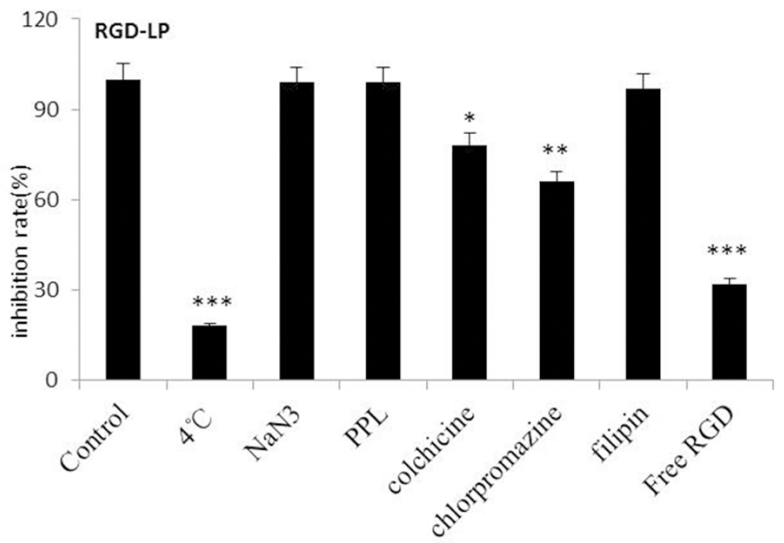

Figure 3. Effects of endocytosis inhibitors on the cellular uptake of liposomes in PC-3 cells. The data are presented as the mean ± SD (n = 3), *P < 0.05, **P < 0.01, ***P < 0.001.

about 3.2 times higher than that of LP, respectively. Indicating that the integrin receptors were also highly expressed on DU145 cells and it is lower than PC-3 cells. The cellular uptake results were consistent with the integrin expression levels on cell surface, indicating that the RGD motif had the ability to recognize and target integrin receptors expressed on the surface of cells.

In order to explore the endocytosis pathways for RGD modified liposomes, endocytosis inhibition assay was conducted. To determine the possible involvement of different endocytic pathways in the cellular uptake of liposomes in PC-3 cells, several classical inhibitors of endocytosis were used, and the fluorescence of cells treated with the different liposomal formulations without any inhibitor was set as 100% and as the control. As shown in **Figure 3**, the uptake of RGD-LP was decreased about 82% ($P < 0.001$) in comparison to control at 4°C. NaN_3 and poly-L-lysine (PPL) did not significantly change the cellular uptake of RGD-LP, indicating that the cellular uptake of RGD-LP was not dependent on energy and charge. The uptake of RGD-LP was decreased about 22% ($P < 0.05$) after incubation with colchicine. Colchicine was known to inhibit the formation of microfilaments and microtubule; therefore, it had an effect on macropinocytosis-mediated uptake. The small effect of colchicine on the uptake of RGD-LP showed that macropinocytosis was presumably involved to a lesser extent. At the same time, by preventing the recycling of clathrin and hindering endocytosis through clathrin-dependent mechanisms with the cationic amphiphilic drug chlorpromazine, a significant decrease (34%, $P < 0.01$) in cellular uptake of RGD-LP was observed in the presence of chlorpromazine, suggesting that the clathrin-dependent pathway was involved in the internalization of RGD-LP. The cellular uptake of RGD-LP did not significantly change with the caveolae-dependent endocytosis inhibitor filipin. These results suggested that the cellular uptake of these liposomes was determined by the combination of various endocytic pathways. The uptake of RGD-LP was

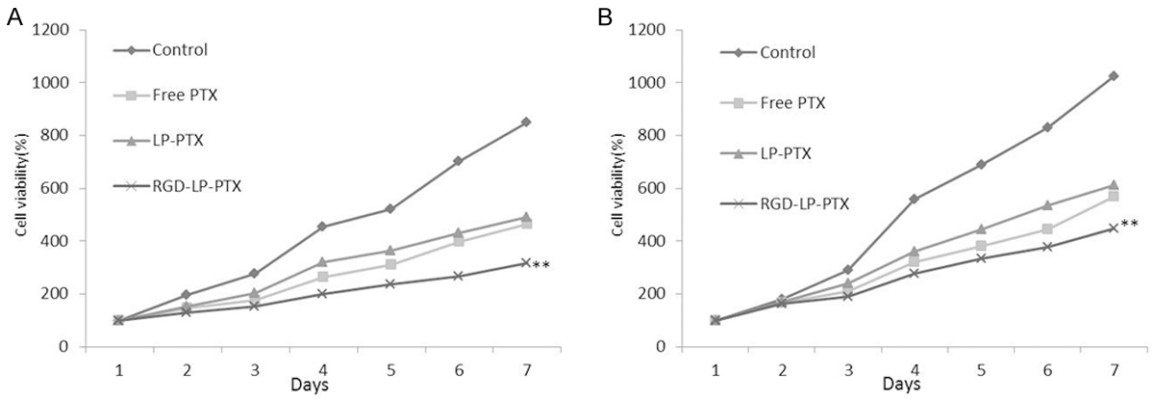

Figure 4. The anti-proliferation of different PTX formulations on tumor cells. A. PC-3 cells; B. DU145 cells. Data are shown as mean ± SEM (n = 3), compare to control group, free PTX group and LP-PTX group, **P < 0.01.

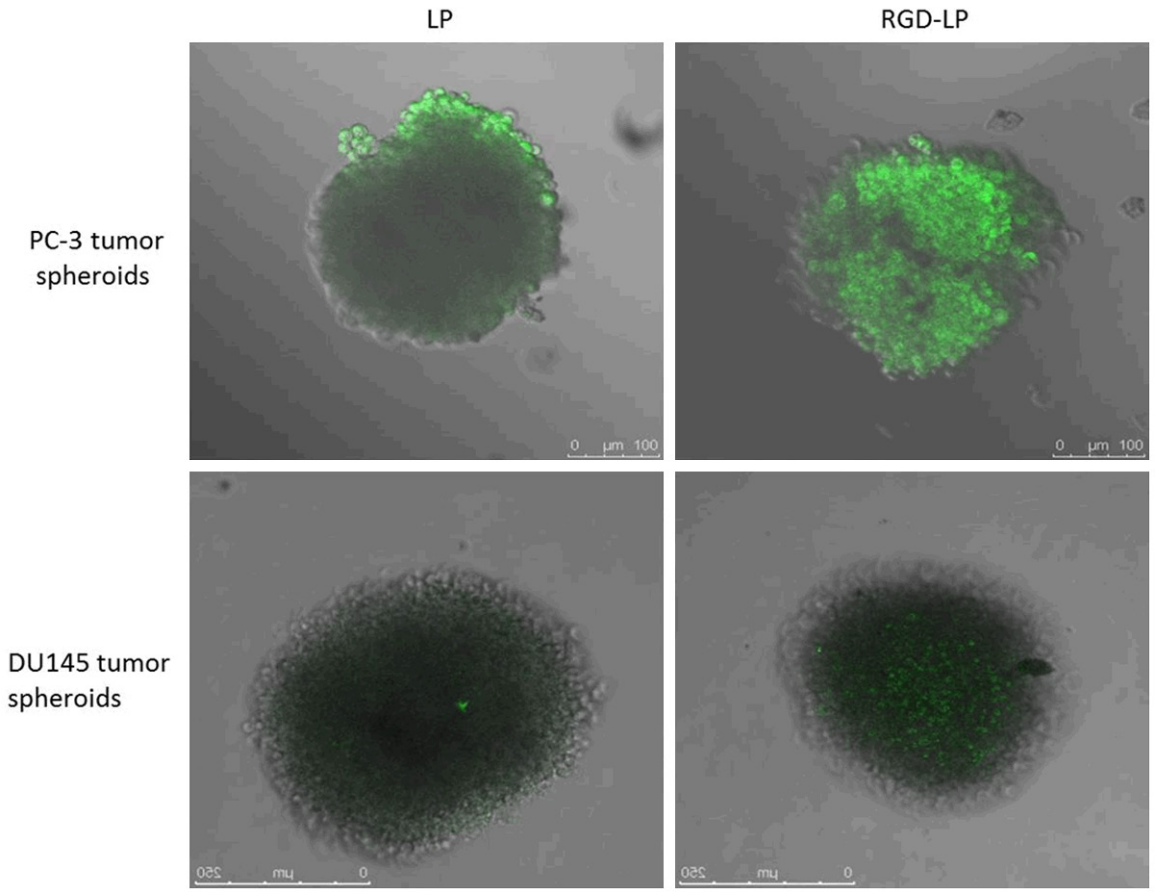

Figure 5. Confocal laser scanning microscopy (CLSM) images show the internalization of fluorescent liposome in PC-3 cells and DU145 cells.

decreased about 68% (P < 0.001) after incubation with free RGD peptide, suggesting that there was competitive inhibition and RGD-LP was internalized into the cells via specific receptors.

RGD-LP-PTX inhibits cell proliferation

PC-3 Cells were incubated with empty vectors were used as a negative control. **Figure 4A** reveal that subsequent to a 7-day period, cell

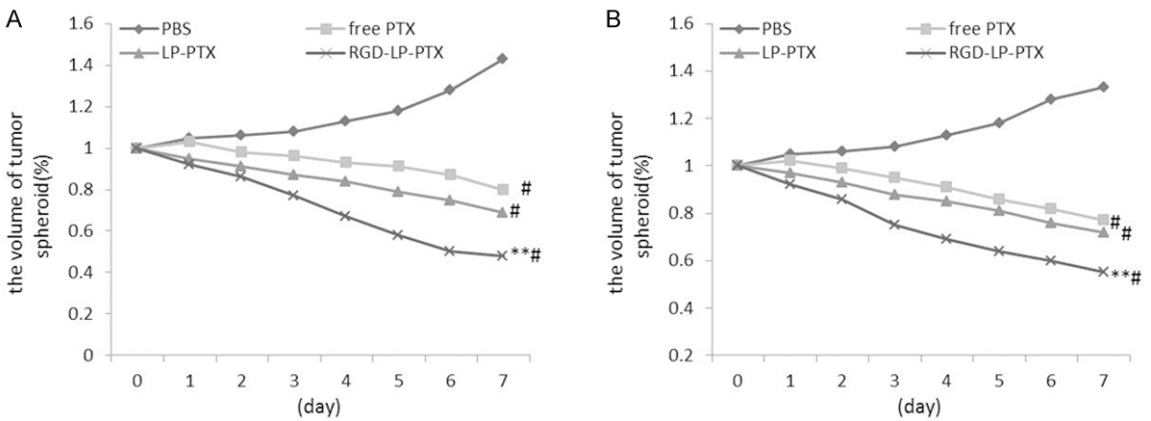

Figure 6. Change ratios of tumor spheroid volume (%) after applying various PTX formulations and blank control, compare to PBS group,#P < 0.01; compare to free PTX group and LP-PTX group, **P < 0.01. A. PC-3 cells. B. DU145 cells.

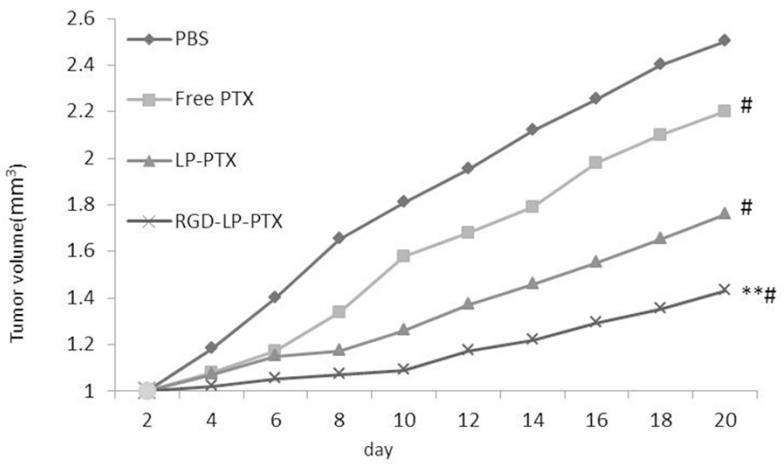

Figure 7. *In vivo* anti-tumor effect of different PTX formulations in PC-3 bearing mice compare to PBS group, #P < 0.01; compare to free PTX group and LP-PTX group, **P < 0.01.

proliferation ability was lower in the RGD-LP-PTX groups than in the LP-PTX and free PTX groups. The remarkable decrease was firstly observed on day 3. Similar results were obtained in DU145 cells, with the results showing in **Figure 4B**.

Evaluation of penetration and growth inhibition of tumor spheroid

Figure 5 shows confocal laser scanning microscopic images of 3D tumor spheroids 8 h. The LP almost entirely lacked efficient penetrating on PC-3 cells and DU145 cells spheroids, indicating that the liposomes without modification had very weak penetration. However, an apparent enhanced fluorescence of the RGD-LP was observed, suggesting that solid tumor penetration was enhanced by the synergistic effect of RGD.

The influence of various treatments on the growth of tumor spheroids was also studied. **Figure 6A**, **6B** represent the in vitro tumor spheroid volume ratios after treatment with PBS, free PTX, LP-PTX and RGD-LP-PTX at the final PTX concentration of 3 mg/ml, respectively. It was observed that tumor spheroids continued to grow in size and volume in the absence of any drug after 7 days. The obvious reduction in volume of tumor spheroids was observed for all PTX formulations after 7 days treatment, indicating that tumor spheroids were sensitive to PTX.

In vivo tumor growth inhibition study

The antitumor effects of PTX-loaded formulations were evaluated on PC-3 tumor xenografts models on BALB/C nude mice. Compared with the rapid tumor volume growth in PBS group, other groups all exhibited tumor inhibition to different extents (**Figure 7**). Free PTX and LP-PTX displayed moderate improvement in the tumor inhibition, while RGD-LP-PTX all exhibited even more outstanding tumor inhibition effect, emphasizing again the importance of

adequate accumulation of drugs into tumors via EPR effect. RGD-LP-PTX exhibited more significant tumor growth inhibition compared with other PTX formulations.

Discussions

There are many barriers to achieve effective targeting efficiency using nanocarrier [29]. Stability in the bloodstream and specific cellular uptake by the target tissues and organs are major obstacles. Liposomes are well-recognized drug delivery vehicles that utilize the fusion of their phospholipid bilayer membrane to the cellular plasma membrane to enhance the delivery and subsequent therapeutic activity of anticancer drugs [30]. However, conventional liposomes are rapidly cleared by the reticular endothelial system *in vivo*. Furthermore, liposomes interact with plasma proteins, resulting in poor specific targeting and a short circulation time. An efficient drug delivery system is needed that can 1) protect drugs from clearance and degradation to keep sufficient circulation-action time *in vivo*, 2) suppress nonspecific uptake by normal or non-target tissues, 3) mediate accumulation of drugs within the target tissues and cells. RGD-based targeting has been successfully used to deliver drugs, biologicals, viruses, nanoparticles, and bioconjugates to tumor [31-33].

The present study describes the preparation and characterization of liposome that binds to Rvâ3 and Rvâ5 integrins via an Arg-Gly-Asp sequence. We coupled this RGD chemically to liposome and demonstrated that such RGD modified liposome conjugates bind to prostatic cancer cells with dramatically increased affinity. Since the binding of the RGD notified liposome can be inhibited by the free RGD, we concluded that RGD notified liposome bind to the cells via the coupled RGD groups.

In the cell uptake experiment, PC-3 cells and DU145 cells were chosen as the targeting cells in vitro because the over-express of Rvâ3 and Rvâ5 integrins on the surface of the cells. Hela cells were used as negative cells without integrin express in the cells. The results (**Figure 3**) showed that the uptake of RGD-LP by PC-3 cells and DU145 cells were marginally greater than that of the LP, which suggested RGD have a high binding affinity for both PC-3 cells and DU145 cells. In Hela cells, αvβ3 integrin are not overexpressed, and RGD could not recognize the Hela cells. The endocytosis pathways for RGD modified liposomes experiment demonstrate the cell uptake of RGD modified liposome was determined by the combination of various endocytic pathways. In the cytotoxicity experiment, the PTX-loaded LP and RGD-LP demonstrated time-and dose-dependent cytotoxic activity towards PC-3 cells and DU145 cells. That was the same with the cell uptake.

In numerous solid tumors, there are regions with high pressure and few vessels [34]. Due to the poor permeation of delivery systems, the level of drug that is able to access the inner area of solid tumors is low [35, 36]. As a consequence, these chemotherapy 'blind areas' eventually and ineluctably induce the recurrence of cancer, and the overall chemotherapeutic efficacy of anticancer agents is compromised. For a cancer treatment to be curative, the delivery system must efficiently penetrate the tumor tissue to reach all of the viable cells [37, 38]. Thereby, three-dimesnional multicellular modeling, which represents the avascular regions found in numerous solid tumor tissues, can serve as an invaluable tool to evaluate the solid tumor penetration effect of a drug delivery system. In the present study, the results demonstrated the penetration capabilities of LP and RGD-LP. It was found that the uptake of RGD-LP, which was higher than that of LP. The RGD could increase the uptake and penetration of RGD-LP by the PC-3 cells and DU145 cells spheroids. These findings indicated that the modification of RGD was able to effectively transport the liposome to the tumor. In the growth inhibition experiments in the present study, utilizing PTX-loaded LP and RGD-LP, the tumor spheroid was used to imitate the *in vivo* status of the solid tumor and to evaluate the antitumor efficiency of the different PTX. The results showed that PTX-loaded RGD-LP possessed the greatest antitumor activity, which may benefit from its increased penetration and uptake by tumors. The modified RGD also could facilitate the transportation of liposomes through tumor spheroids, which was markedly better than LP alone. This finding demonstrated that RGD-LP could overcome the barriers of tumor cells to arrive at the center of the tumor. The anti-tumor effect of PTX-loaded RGD-LP also showed the best efficiency in vivo.

In conclusion, we successfully developed the targeting liposomes modified with the specific

ligand RGD. This liposomal delivery system possessed increased cellular uptake efficiency and targeting specificity in PC-3 cells and DU145 cells whose integrins expression levels were high, and achieved an efficient targeted delivery of payload into tumor cells in PC-3 tumor bearing nude mice and ultimately achieved excellent therapeutic efficacy on tumor-bearing mice. Based on all the studies in this report, we claimed the RGD modified liposomes as a potential anti-tumor drug delivery system.

Disclosure of conflict of interest

None.

Address correspondence to: Xiaozhou He, Department of Urology, Third Affiliated Hospital of Soochow University, 185 Juqian Road, Changzhou 213003, China. E-mail: hexiaozhoucz@163.com

References

[1] Yamamichi F, Matsuoka T, Shigemura K, Kawabata M, Shirakawa T, Fujisawa M. Potential establishment of lung metastatic xenograft model of androgen receptor-positive and androgen-independent prostate cancer (C4-2B). Urology 2012; 80: 951.

[2] Chen W, Wang GM, Guo JM, Sun LA, Wang H. NGF/gamma-IFN inhibits androgen-independent prostate cancer and reverses androgen receptor function through downregulation of FGFR2 and decrease in cancer stem cells. Stem Cells Dev 2012; 21: 3372-3380.

[3] Xiao LJ, Chen YY, Lin P, Zou HF, Lin F, Zhao LN, Li D, Guo L, Tang JB, Zheng XL, Yu XG. Hypoxia increases CX3CR1 expression via HIF-1 and NFkappaB in androgen-independent prostate cancer cells. Int J Oncol 2012; 41: 1827-1836.

[4] Zhang X, Tang Z, Qi L, Chen H, Luo Q. [Screening of membrane antigen differentially expressed in androgen-dependent prostate cancer and androgen-independent prostate cancer]. Zhong Nan Da Xue Xue Bao Yi Xue Ban 2012; 37: 817-823.

[5] Chhipa RR, Wu Y, Mohler JL, Ip C. Survival advantage of AMPK activation to androgen-independent prostate cancer cells during energy stress. Cell Signal 2010; 22: 1554-1561.

[6] Thamilselvan V, Menon M, Thamilselvan S. Carmustine enhances the anticancer activity of selenite in androgen-independent prostate cancer cells. Cancer Manag Res 2012; 4: 383-395.

[7] Venkatesh K, Govindaraj S, Ramachandran A, Kalimuthu S, Perumal E, Velayutham S, Jagadeesan A. Effect of Ukrain on cell survival and apoptosis in the androgen-independent prostate cancer cell line PC-3. J Environ Pathol Toxicol Oncol 2011; 30: 11-19.

[8] Gravina GL, Marampon F, Giusti I, Carosa E, Di Sante S, Ricevuto E, Dolo V, Tombolini V, Jannini EA, Festuccia C. Differential effects of PXD101 (belinostat) on androgen-dependent and androgen-independent prostate cancer models. Int J Oncol 2012; 40: 711-720.

[9] Lian J, Ni Z, Dai X, Su C, Smith AR, Xu L, He F. Sorafenib sensitizes (-)-gossypol-induced growth suppression in androgen-independent prostate cancer cells via Mcl-1 inhibition and Bak activation. Mol Cancer Ther 2012; 11: 416-426.

[10] Morikawa Y, Koike H, Sekine Y, Matsui H, Shibata Y, Ito K, Suzuki K. Rapamycin enhances docetaxel-induced cytotoxicity in a androgen-independent prostate cancer xenograft model by survivin downregulation. Biochem Biophys Res Commun 2012; 419: 584-589.

[11] Guo YJ, Wang LJ, Peng LV, Zhang P. Transferrin-conjugated doxorubicin-loaded lipid-coated nanoparticles for the targeting and therapy of lung cancer. Oncol lett 2015; 9: 1065-1072.

[12] Qin L, Wang CZ, Fan HJ Zhang CJ, Zhang HW, Lv MH, Cui SD. A dual-targeting liposome conjugated with transferrin and arginine glycine aspartic acid peptide for glioma-targeting therapy. Oncol lett 2014; 8: 2000-2006,

[13] Qin Y, Chen H, Zhang Q, Wang X, Yuan W, Kuai R, Tang J, Zhang L, Zhang Z, Zhang Q, Liu J, He Q. Liposome formulated with TAT-modified cholesterol for improving brain delivery and therapeutic efficacy on brain glioma in animals. Int J Pharm 2011; 420: 304-312.

[14] Gao H, Qian J, Cao S, Yang Z, Pang Z, Pan S, Fan L, Xi Z, Jiang X, Zhang Q. Precise glioma targeting of and penetration by aptamer and peptide dual-functioned nanoparticles. Biomaterials 2012; 33: 5115-5123.

[15] Miyata S, Kawabata S, Hiramatsu R, Doi A, Ikeda N, Yamashita T, Kuroiwa T, Kasaoka S, Maruyama K, Miyatake S. Computed tomography imaging of transferrin targeting liposomes encapsulating both boron and iodine contrast agents by convection-enhanced delivery to F98 rat glioma for boron neutron capture therapy. Neurosurgery 2011; 68: 1380-1387.

[16] Du W, Fan Y, Zheng N, He B, Yuan L, Zhang H, Wang X, Wang J, Zhang X, Zhang Q. Transferrin receptor specific nanocarriers conjugated with functional 7peptide for oral drug delivery. Biomaterials 2013; 34: 794-806.

[17] Qin Y, Chen H, Yuan W, Kuai R, Zhang Q, Xie F, Zhang L, Zhang Z, Liu J, He Q. Liposome formulated with TAT-modified cholesterol for enhancing the brain delivery. Int J Pharm 2011; 419: 85-95.

[18] Zhang Q, Tang J, Fu L, Ran R, Liu Y, Yuan M, He Q. A pH-responsive a-helical cell penetrating peptide-mediated liposomal delivery system. Biomaterials 2013; 34: 7980-7993.
[19] Li, S, Wei, J, Yuan, L, Sun H, Liu Y, Zhang Y, Li J, Liu X. RGD-modified endostatin peptide 30 derived from endostatin suppresses invasion and migration of HepG2 cells through the avb3 pathway. Cancer Biother Radiopharm 2011; 26: 529-538.
[20] Kibria G, Hatakeyama H, Ohga N, Hida K, Harashima H. Dual-ligand modification of PEGylated liposomes shows better cell selectivity and efficient gene delivery. J Control Release 2011; 153: 141-148.
[21] Oba M, Fukushima S, Kanayama N, Aoyagi K, Nishiyama N, Koyama H, Kataoka K. Cyclic RGD peptide-conjugated polyplex micelles as a targetable gene delivery system directed to cell spossessing alphavbeta3 and alpha vbeta5 integrins. Bioconjug Chem 2007; 18: 1415-1423.
[22] Jiang X, Xin H, Gu J, Xu X, Xia W, Chen S, Xie Y, Chen L, Chen Y, Sha X, Fang X. Solid tumor penetration by integrin-mediated pegylated poly (trimethylene carbonate) nanoparticles loaded with paclitaxel. Biomaterials 2013; 34: 1739-1746.
[23] Mei DY, Gao HL, Gong W, et al. Anti-glioma effect of doxorubicin loaded liposomes modified with angiopep-2. African Journal of Pharmacy and Pharmacology 2011; 5: 409-414
[24] Sharma G, Modgil A, Sun C, Singh J. Grafting of cell-penetrating peptide to receptor-targeted liposomes improves their transfection efficiency and transport across blood-brain barrier model. J Pharm Sci 2012; 101: 2468-2478.
[25] Jiang T, Zhang Z, Zhang Y, Lv H, Zhou J, Li C, Hou L, Zhang Q. Dual-functional liposomes based on pH-responsive cell-penetrating peptide and hyaluronic acid for tumor-targeted anticancer drug delivery. Biomaterials 2012; 33: 9246-9258.
[26] Maeda N, Takeuchi Y, Takada M, Sadzuka Y, Namba Y, Oku N. Anti-neovascular therapy by use of tumor neovasculature-targeted long-circulating liposome. J Control Release 2004; 100: 41-52.
[27] Chiu SJ, Liu S, Perrotti D, Marcucci G and Lee RJ. Efficient delivery of a Bcl-2-specific antisense oligodeoxyribonucleotide (G3139) via transferrin receptor-targeted liposomes. J Control Release 2006; 112: 199-207.
[28] Kurohane K, Namba Y and Oku N. Liposome modified with a synthetic Arg-Gly-Asp mimetic inhibit lung metastasis of B16BL6 melanoma cells. Life Sci 2000; 68: 273-281.
[29] Liu Y, Li K, Pan J, Liu B, Feng SS. Folic acid conjugated nanoparticles of mixed lipid monolayer shell and biodegradable polymer core for targeted delivery of Docetaxel. Biomaterials 2010; 31: 330-338.
[30] Lewis CE and Pollard JW. Distinct role of macrophages in different tumor microenvironments. Cancer Res 2006; 66: 605-612.
[31] Fukumura D, Xu L, Chen Y, Gohongi T, Seed B and Jain RK. Hypoxia and acidosis independently up-regulate vascular endothelial growth factor transcription in brain tumors in vivo. Cancer Res 2001; 61: 6020-6024.
[32] McNeeley K, Karathanasis E, Annapragada A, Bellamkonda R. Masking and triggered unmasking of targeting ligands on nanocarriers to improve drug delivery to brain tumors. Biomaterials 2009; 30: 3986-3995.
[33] Kuai R, Yuan W, Qin Y, Chen H, Tang J, Yuan M, Zhang Z, He Q. Efficient delivery of payload into tumor cells in a controlled manner by TAT and thiolytic cleavable PEG co-modified liposomes. Mol Pharm 2010; 7: 1816-1826.
[34] Jiang T, Zhang Z, Zhang Y, Lv H, Zhou J, Li C, Hou L, Zhang Q. Dual-functional liposomes based on pH-responsive cell-penetrating peptide and hyaluronic acid for tumor-targeted anticancer drug delivery. Biomaterials 2012; 33: 9246-9258.
[35] Maeda N, Takeuchi Y, Takada M, Sadzuka Y, Namba Y, Oku N. Anti-neovascular therapy by use of tumor neovasculature-targeted long-circulating liposome. J Control Release 2004; 100: 41-52.
[36] Kobayashi H, Man S, Graham CH, Kapitain SJ, Teicher BA and Kerbel RS. Acquired multicellular-mediated resistance to alkylating agents in cancer. Proc Natl Acad Sci U S A 1993; 90: 3294-3298.
[37] Du J, Lu WL, Ying X, Liu Y, Du P, Tian W, Men Y, Guo J, Zhang Y, Li RJ, Zhou J, Lou JN, Wang JC, Zhang X, Zhang Q. Dual-targeting topotecan liposomes modified with tamoxifen and wheat germ agglutinin significantly improve drug transport across the blood-brain barrier and survival of brain tumor-bearing animals. Mol Pharm 2009; 6: 905-917.
[38] Jain RK. Delivery of molecular and cellular medicine to solid tumors. Adv Drug Deliv Rev 2001; 46: 149-168.